AGU PUBLICATIONS

Geophysical Research Letters

RESEARCH LETTER
10.1002/2016GL069652

Key Points:
- First reporting of the Kuroshio being separated into two branches
- The Kuroshio bifurcation results in two warm tongues to the east of the Luzon Strait
- The variability of the eastern branch is associated with Pacific mesoscale eddies

Correspondence to:
G. Wang,
wghocean@yahoo.com

Citation:
Sun, R., G. Wang, and C. Chen (2016), The Kuroshio bifurcation associated with islands at the Luzon Strait, *Geophys. Res. Lett.*, *43*, 5768–5774, doi:10.1002/2016GL069652.

Received 18 MAY 2016
Accepted 18 MAY 2016
Accepted article online 20 MAY 2016
Published online 4 JUN 2016

The Kuroshio bifurcation associated with islands at the Luzon Strait

Ruili Sun[1,2], Guihua Wang[3], and Changlin Chen[3]

[1]State Key Laboratory of Satellite Ocean Environment Dynamics, Second Institute of Oceanography, State Oceanic Administration, Hangzhou, China, [2]College of Physical and Environmental Oceanography, Ocean University of China, Qingdao, China, [3]Institute of Atmospheric Sciences, Department of Environmental Science and Engineering, Fudan University, Shanghai, China

Abstract Based upon a suite of satellite and hydrology data along with numerical model simulations, the Kuroshio is found to be separated into two branches. The two branches are located on the western and eastern sides of the Batanes Islands. The western branch, which is the main branch of the Kuroshio, is estimated to carry roughly 68% of the transport, while the eastern branch, which has not been reported before, carries the remainder. Both branches bring warmer water northward, producing two separate warm tongues east of the Luzon Strait. The western warm tongue has an obvious seasonal variation due to the seasonal variation of the Kuroshio in the northern Luzon Strait, while the eastern warm tongue is associated with Pacific mesoscale eddies. As an anticyclonic (a cyclonic) eddy approaches the Batanes Islands from the east, the eastern branch of the Kuroshio is strongly intensified (weakened), and a more (less) pronounced warm tongue is induced. Consequently, interannual variability of Pacific mesoscale eddies affects the strength of the eastern branch.

1. Introduction

The Kuroshio is one of the strongest western boundary currents in the subtropical oceans. It originates from the North Equatorial Current, passes to the east of the Luzon Strait, flows north into the East China Sea, and returns to the Pacific through the Tokara Strait. Because the Kuroshio transports enormous amounts of heat and volume from the low latitudes to the midlatitudes, it strongly impacts the circulation in the China Seas, downstream currents, regional and global climate, and the fisheries ecosystem [e.g., *Waseda*, 2003; *Tokinaga et al.*, 2009; *Kelly et al.*, 2010; *Qiu et al.*, 2014].

Because of the important roles that the Kuroshio plays in the circulation of the South China Sea (SCS) and beyond, the behavior of the Kuroshio at the Luzon Strait has attracted the attention of many scientists [e.g., *Hu et al.*, 2001; *Yuan et al.*, 2006; *Liang et al.*, 2008; *Lu and Liu*, 2013, to name a few]. Among these studies, three issues have been specifically discussed: (1) the pattern of the Kuroshio intrusion into the SCS [*Farris and Wimbush*, 1996; *Ho et al.*, 2004; *Xue et al.*, 2004; *Caruso et al.*, 2006], (2) the interaction between the Kuroshio and mesoscale eddies [*Jia and Liu*, 2004; *Sheu et al.*, 2010; *Lu and Liu*, 2013], and (3) the interaction of the Kuroshio with topography in numerical simulations [*Metzger and Hurlburt*, 2001; *Lu and Liu*, 2013]. Due to the very complex ocean circulation in the vicinity of the Luzon Strait, almost all these issues are still being studied and openly debated.

Due to the northward transport of warm tropical water by the Kuroshio, the sea surface temperature (SST) around the Luzon Strait has a distinct warm water tongue extending from south to north. This has long been considered the primary SST pattern at the Luzon Strait [*Ho et al.*, 2004] (also see Figure 1a). Recently, we re-examined the SST distribution around the Luzon Strait using 9 km resolution satellite observations. It was found that there were two warm tongues present at the Luzon Strait (Figure 1b). Besides the traditional western warm tongue, discussed in many studies, there was a distinct warm tongue east of the Batanes Islands, which to our best knowledge has not been previously reported. The question then becomes: what causes the two warm tongues and how do they vary? In this study we conclude that the Kuroshio bifurcation associated with the islands drives the formation of the two warm tongues and that anticyclonic (cyclonic) eddies in the Pacific can enhance (weaken) the eastern warm tongue.

2. Data and Models

2.1. Data

The SST from the Remote Sensing System (RSS SST hereafter) (ftp://ftp.discover-earth.org/sst/daily/mw_ir/) has a spatial resolution of 9 km × 9 km, and temporal sampling frequency of 1 day. The data set is merged with

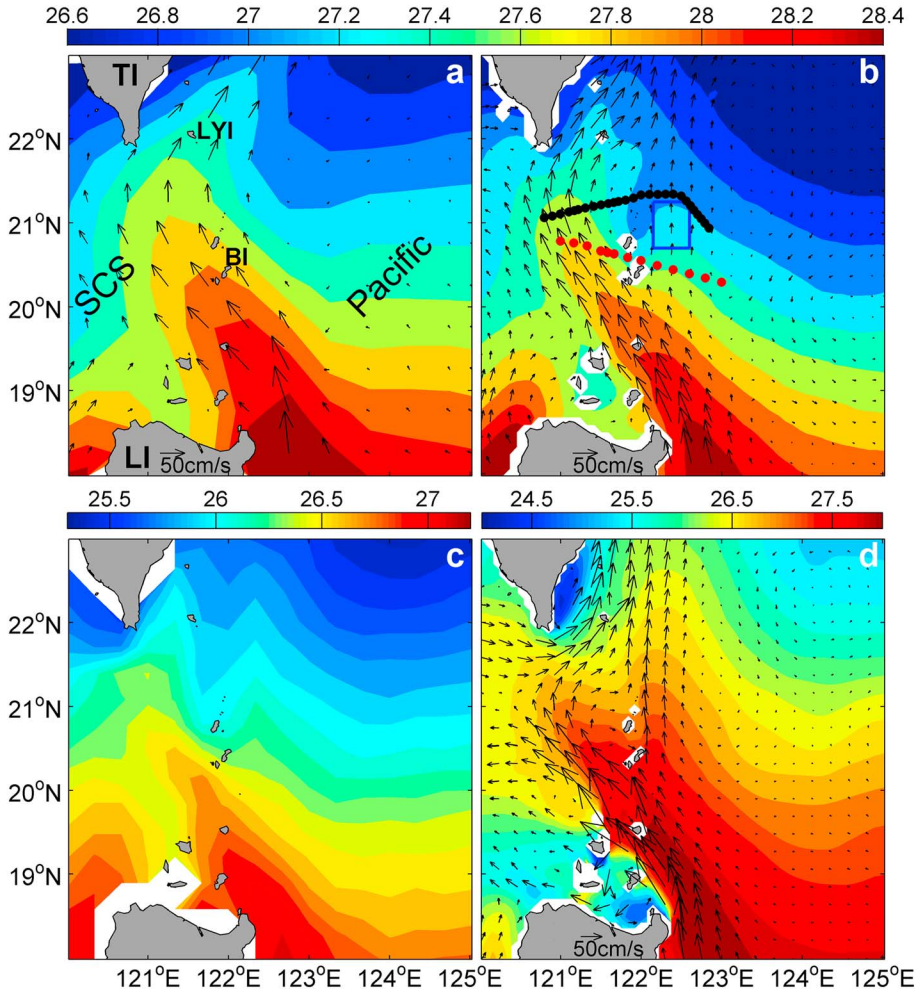

Figure 1. (a) SODA SST (°C; shading) and surface currents (cm/s; vectors) averaged from 1950 to 2007. TI: Taiwan Island, LI: Luzon Island, SCS: South China Sea, BI: Batanes Islands, LYI: Lanyu Island. (b) Satellite SST (°C; shading) and AVISO geostrophic current (cm/s; vectors) averaged from 2006 to 2013. The red dotted line indicates the XBT profile taken on 25 August 2006, and the black dotted line indicates the ADCP profile from January 2003. The blue box extends from 20.70°N to 21.25°N and from 122.25°E to122.65°E. (c) Snapshot SST (°C; shading) simulated by the mixed layer model. (d) Climatological SST (°C; shading) and surface current (cm/s; vectors), simulated by the ROMS model.

infrared measurements from the Moderate Resolution Imaging Spectroradiometer and Microwave measurements from the Advanced Microwave Scanning Radiometer for Earth Observing System, Tropical Rainfall Measuring Mission Microwave Images, and WindSAT. It provides daily data from 12 December 2005 to the present.

The vertical temperature profiles are from Expendable Bathythermograph (XBT) data from May 1989 to December 2011, which is provided by the Global Temperature and Salinity Profile Program (GTSPP, http://www.nodc.noaa.gov/GTSPP/gtspp-home.html) [*Gilson et al*., 1998]. The temperature profile data have been processed to ensure data quality. The XBT profiles extend down to about 800 m with horizontal spacing of roughly 10 profiles per degree of longitude across the Kuroshio. The XBT profiles from 25 August 2006 were selected for this study because they best reflected the Kuroshio bifurcation phenomenon.

The Simple Ocean Data Assimilation (SODA; http://iridl.ldeo.columbia.edu/SOURCES/.CARTON-GIESE/.SODA/.v2p2p4/) [*Carton and Giese*, 2008] product is a monthly mean global ocean reanalysis data set with a spatial resolution of 0.5° × 0.5° on 40 standard levels from the surface down to 5375 m depth.

The geostrophic current, geostrophic current anomaly, and sea surface height anomaly (ftp://ftp.aviso.oceanobs.com/) are provided by the Archiving Validation and Interpretation of Satellite Data in Oceanography

(AVISO) [*Ducet et al*., 2000]. The AVISO product is a merged one using the TOPEX/Poseidon, European Remote Sensing, and Jason-1 satellites observational data. It provides daily data from 1 January 1993 to 31 May 2014 with a spatial resolution of 0.25° × 0.25°. In addition, the Acoustic Doppler Current Profiler (ADCP) data are provided by China Argo Real-time Data Center (ftp://ftp.argo.org.cn/pub/adcp/). The cruise was employed by January 2003, and the data sample layers are 25–50 m, 50–75 m, 75–100 m, 100–125 m, and 125–150 m.

2.2. Models

A simple mixed-layer model is used in this study. The mixed layer temperature equation is the same as that in *Qu* [2001], except that only the geostrophic component of the advection of mixed layer temperature is included. Consequently, the equation for the temperature evolution is

$$\frac{\partial T}{\partial t} = -\left(u_g \frac{\partial T}{\partial x} + v_g \frac{\partial T}{\partial y}\right)$$

where T is the SST or the mixed layer temperature; t is time; x and y are the conventional east-west and north–south Cartesian coordinates, respectively; and u_g and v_g are the x and y components of the geostrophic velocity, respectively. The geostrophic current is averaged from 2006 to 2013, and the temperature field is initialized with the zonal mean SST in climatology. The horizontal resolution is 1/4°, and the time step is one hour. Note that neither the heat lost to the atmosphere nor the horizontal mixing with the surrounding cold water is included in the model. The model is assumed to have reached equilibrium once the temperature variation between two successive time steps is smaller than 0.1°C.

To consider more complete dynamics, Regional Ocean Modeling System (ROMS) is also applied. The ROMS is a free-surface, terrain-following, primitive equations ocean model [*Shchepetkin and McWilliams*, 2009]. For the present study, the model domain extends from 2°S to 28°N and from 99°E to 142°E, with a horizontal resolution of 1/12°, and there are 30 sigma levels in the vertical direction. The model is integrated for 20 years using monthly climatological heat flux forcing from the Objectively Analyzed air-sea Fluxes [*Yu and Weller*, 2007] and cross-calibrated multiplatform wind stress forcing [*Atlas et al*., 2011]. The monthly climatology of the last 5 years of model output is captured and used for the analysis herein. The specific details of the model configuration can be found in either *Wang et al*. [2013] or *Chen and Wang* [2014].

3. Results

3.1. Identification of the Kuroshio Bifurcation

Figure 1b shows the ocean circulation derived from the satellite altimetry data. As in Figure 1b, there is a strong current along the western side of the Batanes Islands (hereafter the western branch) and a weaker, narrow northward current to the east of the Batanes Islands (hereafter the eastern branch). The average flow speeds are around 0.45 and 0.29 m/s for the western and eastern branches, respectively. The current is weak in between the two branches. The two branches seem to be two currents of a bifurcation. The two branches originate from the Kuroshio to the east of the Philippine Islands and are formed as the Kuroshio impinges upon the Batanes Islands. The western branch, which is the main branch of the Kuroshio, is estimated to carry roughly two thirds of the total transport, while the eastern branch, which has not been reported before, carries the remainder.

Because low-latitude water is usually warmer than that at high latitude, the two northward currents transport warmer water northward. Therefore, to investigate the heat transport of the two branches, a mixed layer model including only geostrophic heat advection is applied to the Luzon Strait. The spatial correlation coefficient between the simulated SST and satellite-observed SST from this geostrophic mixed-layer model is around 0.96, demonstrating that the two warm tongue current branches can reproduce the SST reasonably well (Figure 1c). Further, the implementation of the three-dimensional ROMS model can also produce the bifurcation and associated warm tongues (Figure 1d) with good fidelity. These two models suggest that the Kuroshio bifurcation at the Luzon Strait is a robust feature and leads to the formation of the two warm tongues.

To look at the vertical structures of the two branches and associated warm tongues, an XBT transect passing through the two warm tongues was conducted. In order to cleanly isolate the structure of the two warm tongues, the zonal mean temperature is removed from the data and the results are presented in Figure 2a. Both warm tongues reach to depths deeper than 400 m and possess widths of around 100 km. The deep penetration depths of the temperature anomalies suggest that ocean currents play an important role in

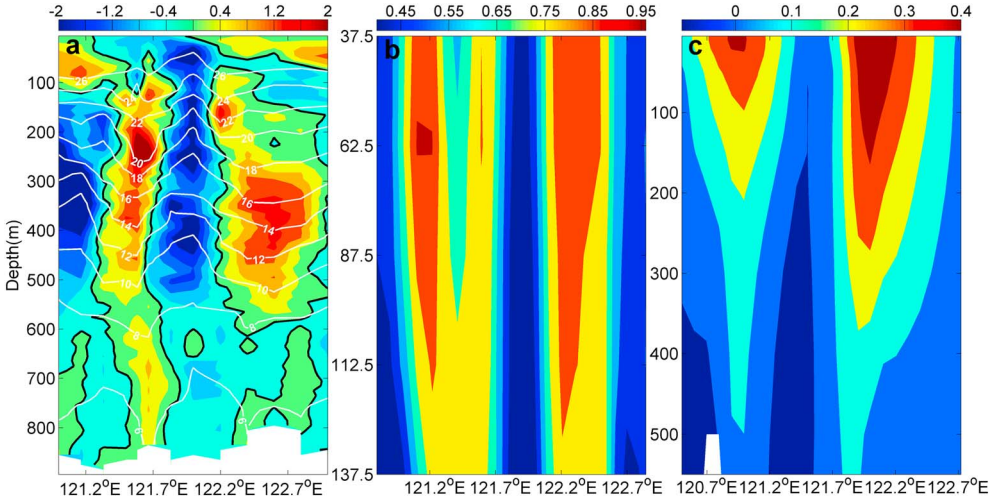

Figure 2. (a) XBT temperature (°C; white contour), and vertical profile of temperature anomaly (°C; shading), with the zonal mean removed. The solid black lines are the zero contours of temperature anomaly. (b) Vertical profile (m/s) of meridional flow speed observed by the ADCP. (c) Climatological vertical profile (m/s) of meridional flow speed simulated by the ROMS model. The *y* axis for all panels is depth (m).

forming the warm tongues. Actually, these two northward currents were also detected in the ADCP transect observation (Figure 2b), with maximum speeds of 0.96 and 0.94 m/s for the western and eastern branches, respectively. The two currents can extend to a few hundred meters. The simulated circulation from high-resolution OGCM also demonstrates the robust feature (Figure 2c).

3.2. Variability of the Kuroshio Bifurcation

Because the two branches flow primarily northward, we use the power spectrum of the meridional current speed as a proxy for monitoring the variability of the two branches of the Kuroshio. It turns out that the intra-seasonal and interannual signals are dominant for the eastern branch (the seasonal signal is very weak in blue box shown in Figure 1b), while the seasonal variaibility is primary for the western branch, in particular, in the north of 20.5°N. To show the seasonal variability of the western branch, we compute composite ocean currents in summer and in winter and present them in Figures 3a and 3b, respectively. In summer, the western branch of the Kuroshio flows to the east of the island of Taiwan without intruding into the SCS, but in winter the intrusion is pronounced after the branch reaches 20.5°N. The circulation difference between summer and winter in the northern flank of the western branch results in a strong seasonal variability there (Figure 3c), which was also discussed by *Qu* [2000] and *Qu et al.* [2004].

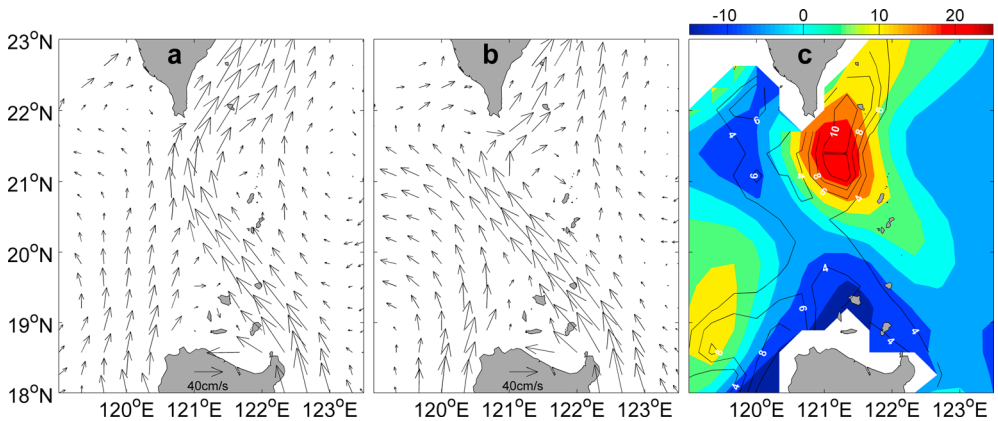

Figure 3. (a) AVISO currents (cm/s; vectors) in summer from 1993 to 2013. (b) Same as Figure 3a, except in winter. (c) The difference in meridional current speed between summer and winter (cm/s; shading), and power spectrum of the seasonal variability of meridional current speed from January 1993 to December 2013 (cm^2/s^2; contour).

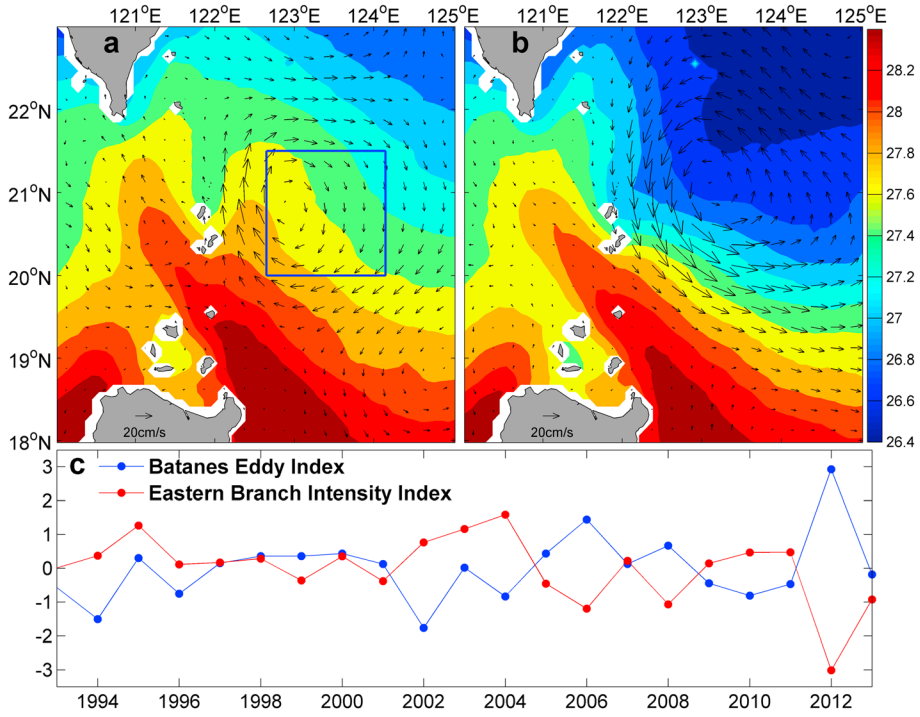

Figure 4. (a) Composition of SST (°C; shading) and geostrophic current anomaly (cm/s; vectors) for positive index days. (b) Same as Figure 4a, except for negative index days. The latitude-longitude limits of the blue box in Figure 4a are 20.0°N–21.5°N, 122.65°E–124.15°E. (c) Batanes Eddy Index (BEI, blue line) and the Eastern Branch Intensity Index (EBII, red line). Both have been normalized.

There is some evidence that the intraseaonal variability of the eastern branch may be due to the action of Pacific mesoscale eddies because the dominant frequency is similar to that of the eddies [*Yang et al.*, 2013]. Using the time series of the meridional current speed in the blue box in Figure 1b as the Eastern Branch Intensity Index (EBII), we composite geostrophic current anomalies and SST (Figures 4a and 4b) based on the days when the positive and negative intensity index values are more than 0.5 standard deviations away from the mean. An anticyclonic (a cyclonic) circulation anomaly and its associated temperature variability are shown in Figure 4a (Figure 4b) for the days of postive (negative) intensity index. As the anticyclonic (cyclonic) eddy approaches the islands, the eastern branch is intensified (weakened), and an enhanced (weakened) warm tongue develops to the east of the Batanes Islands.

The interannual variability of the eastern branch also appears to be related to the action of Pacific mesoscale eddies. Counting the number of days that the center of anticyclonic eddies and cyclonic eddies was located within the blue box in Figure 4a between 1993 and 2013. The size of the blue box is chosen to match the average radius of the mesoscale eddies in the northwestern subtropical Pacific Ocean, which is around 130 km [*Yang et al.*, 2013]. We define the Batanes Eddy Index (BEI) as the number of days that cyclonic eddies occur within the blue box minus the number of days that anticyclonic eddies occur there. Consequently, a positive (negative) BEI indicates more cyclonic (anticyclonic) eddies appearing to the east of the Batanes Islands. Figure 4c shows a superposition of the times series of the BEI and EBII. It is apparent that the two indices are negatively correlated with the correlation coefficient reaching −0.74 at the 95% confidence level. This indicates that as more anticyclonic (cyclonic) eddies appear to the east of the Batanes Islands, the eastern branch of the Kuroshio becomes stronger (weaker).

4. Summary

Using a suite of new satellite and hydrology data in combination with results from numerical simulations, a new feature was revealed: as the Kuroshio encountered the Batanes Islands, it can bifurcate and pass around both sides of the islands, and further produce two warm tongues.

Our results demonstrate that the western branch has obvious seasonal variability north of 20.5°N. This is a reflection of the branch pattern at the Luzon Strait: the intrusion of the Kuroshio into the SCS is less frequent in summer but much more frequent in winter. The eastern branch has strong intraseasonal and interannual variabilities associated with the Pacific mesoscale eddies. As anticyclonic (cyclonic) eddies approach the islands, the eastern branch is intensified (weakened), and a more (less) developed warm tongue is induced to the east of the Batanes Islands.

One remaining question is whether the bifurcation of the Kuroshio can impact the characteristics of the Kuroshio Current downstream? Our preliminary study suggests that the transport of the two branches is nearly a simple superposition of the upstream Kuroshio with the flow field of the mesoscale eddies. As a result, it is expected that the bifurcation can enhance the downstream Kuroshio Current and the associated potential vorticity field. Therefore, the downstream influence of the bifurcation is a topic worthy of further study in the future. As shown in Figure 2c, the simulated eastern tongue is more developed than the western one, which is different from observational data. This may indicate that islands may play the important role in the Kuroshio bifurcation, and therefore the role that the island's size and location play in the Kuroshio bifurcation needs to be investigated with a higher resolution ocean model.

Our study provides some new insights into the variability of the Kuroshio and can help us to further understand the downstream behavior of the Kuroshio and its role in the SCS circulation.

Acknowledgments

The authors wish to acknowledge several community data sets used in this study. The geostrophic current data were obtained from AVISO (ftp://ftp.aviso.oceanobs.com/), the ADCP data were provided by China Argo Real-time Data Center (ftp://ftp.argo.org.cn/pub/adcp/), the SST data were obtained from RSS SST (ftp://ftp.discover-earth.org/sst/daily/mw_ir/), the XBT data came from GTSPP (http://www.nodc.noaa.gov/GTSPP/gtspp-home.html), and the SODA data were obtained from http://iridl.ldeo.columbia.edu. This study was supported by the National Natural Science Foundation of China (41125019), the National Basic Research Program of China (2013CB430301), the NSFC (41576022), and the Chinese Academy of Sciences Strategic Priority Research Program (XDA11020201 and XDA11010103).

References

Atlas, R., R. N. Hoffman, J. Ardizzone, S. M. Leidner, J. C. Jusem, D. K. Smith, and D. Gombos (2011), A cross-calibrated, multiplatform ocean surface wind velocity product for meteorological and oceanographic applications, *Bull. Am. Meteorol. Soc.*, *92*, 157–174.

Carton, J. A., and B. S. Giese (2008), A reanalysis of ocean climate using SODA, *Mon. Weather Rev.*, *136*, 2999–3017.

Caruso, M. J., G. G. Gawarkiewicz, and R. C. Beardsley (2006), Interannual variability of the Kuroshio intrusion in the South China Sea, *J. Oceanogr.*, *62*(4), 559–575.

Chen, C., and G. Wang (2014), Interannual variability of the eastward current in the western South China Sea associated with the summer Asian monsoon, *J. Geophys. Res. Oceans.*, *119*, 5745–5754, doi:10.1002/2014JC010309.

Ducet, N., P. Y. Le Traon, and G. Reverdin (2000), Global high-resolution mapping of ocean circulation from TOPEX/Poseidon and ERS-1 and -2, *J. Geophys. Res.*, *105*, 19,477–19,498, doi:10.1029/2000JC900063.

Farris, A., and M. Wimbush (1996), Wind-induced kuroshio intrusion into the South China Sea, *J. Oceanogr.*, *52*(6), 771–784.

Gilson, J., D. Roemmich, B. Cornuelle, and L. Fu (1998), Relationship of TOPEX/Poseidon altimetric height to steric height and circulation in the North Pacific, *J. Geophys. Res.*, *103*, 27,947–27,965, doi:10.1029/98JC01680.

Ho, C. R., Q. Zheng, N. J. Kuo, C. H. Tsai, and N. E. Huang (2004), Observation of the Kuroshio intrusion region in the South China Sea from AVHRR data, *Int. J. Remote. Sens*, *25*(21), 4583–4591, doi:10.1080/0143116042000192376.

Hu, J., H. Kawamura, H. Hong, F. Kobashi, and D. Wang (2001), 3–6 months variation of sea surface height in the South China Sea and its adjacent ocean, *J. Oceanogr.*, *57*(1), 69–78.

Jia, Y., and Q. Liu (2004), Eddy shedding from the Kuroshio bend at Luzon Strait, *J. Oceanogr.*, *60*(6), 1063–1069.

Kelly, K. A., R. J. Small, R. M. Samelson, B. Qiu, T. M. Joyce, Y. O. Kwon, and M. F. Cronin (2010), Western boundary currents and frontal air-sea interaction: Gulf Stream and Kuroshio Extension, *J. Clim.*, *23*(21), 5644–5667, doi:10.1175/2010jcli3346.1.

Liang, W. D., Y. J. Yang, T. Y. Tang, and W. S. Chuang (2008), Kuroshio in the Luzon Strait, *J. Geophys. Res.*, *113*, C08048, doi:10.1029/2007JC004609.

Lu, J., and Q. Liu (2013), Gap-leaping Kuroshio and blocking westward-propagating Rossby wave and eddy in the Luzon Strait, *J. Geophys. Res. Oceans.*, *118*, 1170–1181, doi:10.1002/jgrc.20116.

Metzger, E. J., and H. E. Hurlburt (2001), The importance of high horizontal resolution and accurate coastline geometry in modeling South China Sea Inflow, *Geophys. Res. Lett.*, *28*, 1059–1062, doi:10.1029/2000GL012396.

Qiu, B., S. Chen, N. Schneider, and B. Taguchi (2014), A coupled decadal prediction of the dynamic state of the Kuroshio Extension system, *J. Clim.*, *27*, 1751–1764.

Qu, T. (2000), Upper-layer Circulation in the South China Sea, *J. Phys. Oceanogr.*, *30*, 1450–1459.

Qu, T. (2001), Role of ocean dynamics in determining the mean seasonal cycle of the South China Sea surface temperature, *J. Geophys. Res.*, *106*, 6943–6955, doi:10.1029/2000JC000479.

Qu, T., Y. Y. Kim, M. Yaremchuk, T. Tozuka, A. Ishida, and T. Yamagata (2004), Can Luzon Strait transport play a role in conveying the impact of ENSO to the South China Sea? *J. Clim.*, *17*(18), 3644–3657.

Shchepetkin, A. F., and J. C. McWilliam (2009), Correction and commentary for "Ocean forecasting in terrain-following coordinates: Formulation and skill assessment of the Regional Ocean Modeling System.", *J. Comput. Phys.*, *228*, 8985–9000, doi:10.1016/j.jcp.2009.09.002.

Sheu, W. J., C. R. Wu, and L. Y. Oey (2010), Blocking and westward passage of eddies in the Luzon Strait, *Deep Sea Res. Part II: Topical Studies in Oceanography*, *57*(19–20), 1783–1791, doi:10.1016/j.dsr2.2010.04.004.

Tokinaga, H., Y. Tanimoto, S. P. Xie, T. Sampe, H. Tomita, and H. Ichikawa (2009), Ocean frontal effects on the vertical development of clouds over the western North Pacific: In situ and satellite observations*, *J. Clim.*, *22*(16), 4241–4260, doi:10.1175/2009jcli2763.1.

Wang, G., Z. Ling, R. Wu, and C. Chen (2013), Impacts of the Madden–Julian Oscillation on the summer South China Sea ocean circulation and temperature, *J. Clim.*, *26*(20), 8084–8096.

Waseda, T. (2003), On the eddy-Kuroshio interaction: Meander formation process, *J. Geophys. Res.*, *108*(C7), 3220, doi:10.1029/2002JC001583.

Xue, H., F. Chai, N. Pettigrew, and D. Xu (2004), Kuroshio intrusion and the circulation in the South China Sea, *J. Geophys. Res.*, *109*. C02017, doi:10.1029/2002JC001724.

Yang, G., F. Wang, Y. Li, and P. Lin (2013), Mesoscale eddies in the northwestern subtropical Pacific Ocean: Statistical characteristics and three-dimensional structures, *J. Geophys. Res. Oceans*, *118*, 1906–1925.

Yu, L., and R. A. Weller (2007), Objectively analyzed air-sea heat fluxes (OAFlux) for the global ice-free oceans (1981–2005), *Bull. Am. Meteorol. Soc.*, *88*, 527–539.

Yuan, D., W. Han, and D. Hu (2006), Surface Kuroshio path in the Luzon Strait area derived from satellite remote sensing data, *J. Geophys. Res.*, 111, C11007, doi:10.1029/2005JC003412.